Proceedings World Geothermal Congress 2020+1
Reykjavik, Iceland, April - October 2021

Towards a Comprehensive Volcanologic, Magmatic and Structural Model for Superhot Geothermal Systems: Case Study of Los Humeros Caldera Complex, Mexico

Gerardo Carrasco-Núñez[1], Gianluca Norini[2], Guido Giordano[3], Federico Lucci[3], Javier Hernández[1], Jaime Cavazos[1], Héctor Cid-Luna[1], Pablo Dávila[4], Daniela Peña[1], Steven Barrios[1], Francisco Fernández[1].

1 Centro de Geociencias, Universidad Nacional Autónoma de México, Campus Juriquilla, Querétaro, 76100, Mexico
2 Istituto per la Dinamica dei Processi Ambientali, CNR, Milano, Italy
3 University of Roma Tre, Roma, Italy
4 IPICYT, San Luis Potosí, Mexico

1 gerardoc@geociencias.unam.mx

Keywords: Geothermal exploration, superhot geothermal systems, geologic model, volcano-structural model, magmatic model, Los Humeros, Mexico

ABSTRACT

Superhot geothermal systems (SHGS) are now important targets for geothermal exploration worldwide. Unraveling how SHGS work is a challenging task that requires a solid geologic knowledge of the studied geothermal system, which includes its volcanologic, magmatic and structural evolution in order to explain how the geothermal system originated and developed through time. The geothermal field of Los Humeros volcanic complex (LHVC) is a classic example of SHGS. It is located in the central-eastern zone of Mexico, and is one of the most important geothermal fields with an installed capacity of ca. 94 MW. Several studies on LHVC exist; however, due to the complexity of the volcano-structural internal structure, there are still open questions that must be addressed to achieve a better understanding of how the magmatic plumbing system works and its relationship with the geothermal field. This paper presents a multidisciplinary set of studies including volcanologic, structural, petrologic and petrophysical approaches that together integrate a preliminary comprehensive model. The formation of the LHVC involved multiple trapdoor, and less piecemeal caldera collapse events. These events occurred over an intricate pre-caldera geologic scenario composed of a highly folded and fractured sedimentary basement filled by a thick sequence of andesitic lava flows, followed by rhyolitic volcanism. As a result, a highly complex internal structure formed at depth, that connected with fracture systems formed during a caldera resurgence stage, and that may constitute the main paths of the geothermal fluids to the surface. The local stress field caused by the injection of new magma during the resurgence stage and the occurrence of hydrothermal fluids in the geothermal reservoir result from the interplay among the heat source (inferred magma intrusion), the recent ground faulting (caldera resurgence) and intense post-calderas volcanic activity. It is possible that the main resurgence faults correspond to the reactivation of the inherited tectonic planes in the basement underlying the LHVC. A polybaric magmatic system, as obtained by inverse thermobarometry models, supports a configuration with multiple magmatic stagnation levels that fed different eruptive phases of the post-caldera stage of LHVC. Although it is clear that fractures are the main control of permeability, an important contribution is provided by primary vesiculation in the matrix (microporosity) of the volcanic rocks. Furthermore, spatial lithofacies variations of the overlying ignimbritic unit (Xáltipan ignimbrite), particularly controlled by primary welding degree and secondary mineralization, must be taken into account, since it produces strong permeability variations, and therefore irregularities on the fluid path of the geothermal reservoir. Recurrent injection of magmas until the Holocene is also associated with a diversification of the magmatic sources and their interaction with the geothermal system. These results point to a more complex geothermal system than previously believed, that requires the correct integration of these studies.

1. INTRODUCTION

Renewable energy resources, such as those related to geothermal systems, are now the focus of intense exploration programs for future sustainability around the world. There is a special interest worldwide to study non-conventional geothermal systems, such as SHGS and enhanced geothermal systems (EGS). For that purpose, a collaborative research consortium between the European Union and Mexico, named as GEMex, is currently developing a comprehensive study on those systems, where the Los Humeros Volcanic Complex (LHVC) has been targeted as a representative case study of a superhot geothermal system. Partial results of this project are shown in this work.

LHVC is a Late Pleistocene-Holocene caldera system hosting an active geothermal field with current installed capacity of electricity is *ca*. 94 MW, occupying the third place in Mexico, after Cerro Prieto (570 MW) and Los Azufres (247 MW). In the last decade, Mexico passed from the third to the sixth position worldwide in the generation of this energy (Gutiérrez-Negrín, 2019), which enhances the current interest of the Mexican government in developing the geothermal energy production of the country. Due to the geothermal interest, LHVC has been extensively studied by different disciplines: surface geology (Pérez-Reynoso, 1978; De la Cruz, 1983; Yáñez and García, 1980; and Ferriz and Mahood, 1984), structural geology (Garduño-Monroy et al., 1985; López-Hernández, 1995; Norini et al., 2015), volcanology and petrology (Carrasco-Núñez and Branney, 2005; Wilcox, 2011; Carrasco-Núñez et al., 2012; Dávila-Harris and Carrasco-Núñez, 2014), geophysical aspects (Palacios-Hertweg and García-Velázquez, 1981; Campos-Enríquez and Garduño-Monroy, 1987; Arredondo et al., 2007; Lermo et al., 2008), geochemistry (Verma, 1983; Ferriz and Mahood, 1987; Verma, 2000), about hydrothermalism (Barragán et al., 1991; Prol, 1998), subsurface geology (Viggiano and Robles, 1988; Cedillo et al., 1994; Cedillo, 1997; Cedillo, 1999; Gutiérrez-Negrín and Izquierdo-Montalvo, 2010; Viggiano and Flores-Armenta, 2008; Lorenzo-Pulido, 2008; and other internal reports), and by conceptual models (Arellano et al., 2003; Gutiérrez-Negrín and Izquierdo-Montalvo, 2010).

Despite all of these works, and due to the intrinsic complexity of the LHVC geologic and volcanic evolution, a detailed characterization of its internal structure is still missing. The complexity of this system is marked by multiple overlapping cataclysmic caldera-forming episodes, followed by episodic intrusions of magma and by a recent resurgence process that create highly heterogeneous conditions to allow the formation of a geothermal reservoir that is currently exploited for an efficient power production. Therefore, in this study we propose an integrated approach for LHVC, combining volcanological, magmatic and structural studies with the aim to understand the relation between the main geothermal parameters such as the heat source, secondary and primary permeability, cap rock characteristics, and recharge conditions, and furthermore to apply this knowledge to increase the geothermal potential of LHVC. Our approach involves extensive field data, analytic work, and the use of geophysical and geochemical analyses to support our interpretations, which at the end allow us to propose an updated and more realistic model of the LHVC.

2. REGIONAL GEOLOGIC SETTING

LHVC is located at the eastern part of the Trans Mexican Volcanic Belt (TMVB), which is mostly originated by the subduction of the Cocos and Rivera plates underneath the North American plate in the Mesoamerican trench (Figure 1) since the Miocene. The caldera structure developed over a singular geological and tectonic context in the Serdán-Oriental basin (SOB). This is a closed basin at the Mexican high plateau, filled by Quaternary sediments, pyroclastic and volcaniclastic deposits, and scattered monogenetic volcanic structures (scoria cones, lava fields, maars and tuff-rings) of basaltic to rhyolitic composition and by several older felsic domes. (Yáñez and García, 1982).

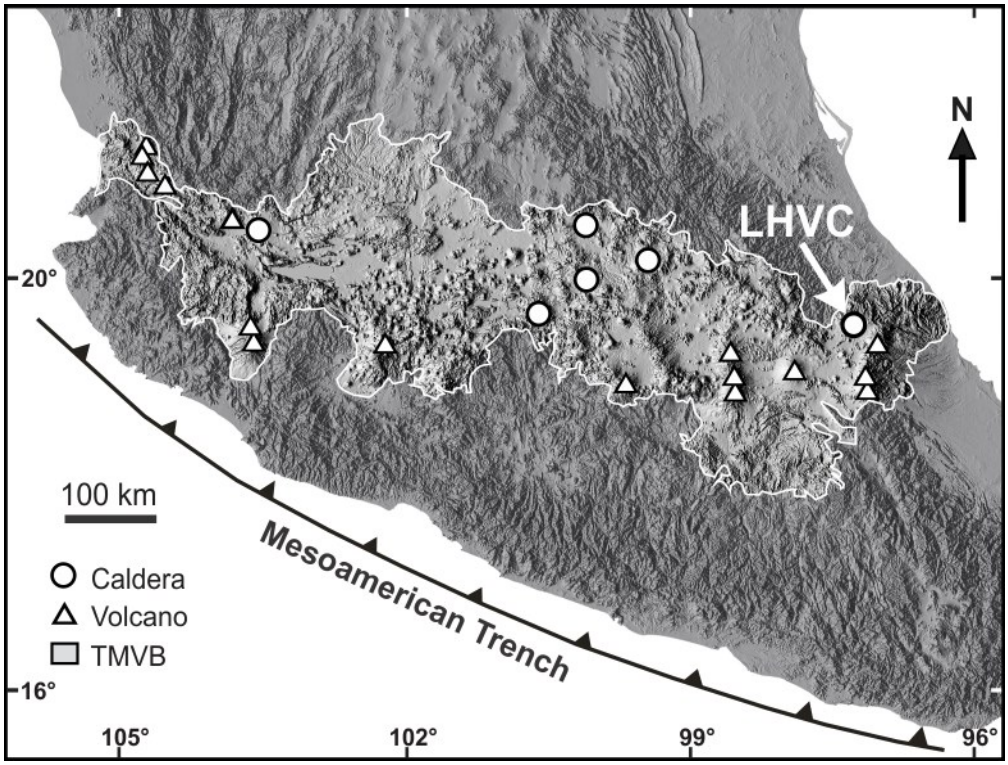

Figure 1: Location of Los Humeros Volcanic complex and geothermal field at the northern part of the Eastern Mexican Volcanic Belt.

Stratigraphically, the oldest units exposed in the area around LHVC form a suite of late Paleozoic intrusive, metamorphic and meta-sedimentary rocks that conforms the Teziutlán Massif (Yáñez and García, 1982). Resting over the metamorphosed basement occurs a thick Mesozoic sedimentary succession composed of red sandstone and shale, marine carbonates, and shaly limestone, (Viniegra-Osorio, 1965). Cutting the basement rocks occurs an Eocene to Oligocene suite of syenitic and granodioritic intrisives, which locally produced marble, skarn and hornfels facies (Yáñez and García, 1982). A subsequent period of extrusive volcanic episodes during Miocene-Pliocene is recorded by intermediate to mafic lavas of the Cerro Grande Complex-Cuyuaco (8.9-10.5 Ma, Yañez and García, 1982; Carrasco-Núñez et al. 1997) and the Alseseca and Teziutlán andesites (recently dated by Ar/Ar at 1.4 to 2.6 Ma (Carrasco-Núñez et al., 2017). The latter unit can be correlated with the pre-caldera volcanism observed at the geothermal wells. Younger scattered volcanism within the Serdán-Oriental basin is characterized by a bimodal composition, including isolated rhyolitic domes such as Cerro Pizarro Cerro Pinto, Las Águilas and Las Derrumbadas, and both basaltic and rhyolitic maars (Aljojuca, Atexcac, Alchichica amongst others) and tuff rings (Tepexitl), as well a small basaltic cinder cones of mostly Pleistocene and Holocene ages (Carrasco-Núñez et al., 2012).

3. VOLCANOLOGICAL EVOLUTION

LHVC has a long, diverse, and complex evolution, that according to Carrasco-Núñez et al. (2017b; 2018), can be divided in three main sequential eruptive stages: a) pre-caldera stage; (b) caldera stage; and (c) post-caldera stage (Figure 2).

3.1 Pre-caldera stage

The pre-caldera stage comprises a period dominated by rhyolitic volcanism (Carrasco-Núñez et al., 2017b), with episodic dome growth volcanism in the area, ranging from 693.0±1.9 Ka ($^{40}Ar/^{39}Ar$, plagioclase; Carrasco-Núñez et al., 2018) to 270±40 ka (U/Th, zircon, Carrasco-Núñez et al., 2018), with some occurrences at 486.5±2.4 and 270±17 ka, and 360±100 ka (K/Ar, sanidine; Ferriz and Mahood, 1984).

3.2 Caldera stage

The Caldera stage is bounded by two caldera-forming eruptions and by a sequence of episodic large Plinian eruptions. The onset of this stage is marked by the largest single-eruption of LHVC that produced an irregular, *ca*.18 km Los Humeros caldera collapse, with the sudden evacuation of large pyroclastic density currents forming the Xaltipan ignimbrite, with an estimated volume of 291 km^3 (dense rock equivalent-DRE) (Cavazos and Carrasco-Núñez, in review). This unit rendered an age of 164.0±4.2 ka recently dated by combined U-Th (zircon) and $^{40}Ar/^{39}Ar$ (plagioclase) dating (Carrasco-Núñez et al. (2018) (Figure 3), which is considerably younger than the previously proposed of 460±20 ka (K/Ar, Ferriz and Mahood, 1984). This new age represents a geothermal system rejuvenation that has important implications in estimating geothermal potential. Variations in welding lithofacies of the Xaltipan ignimbrite both vertical and lateral are recorded in several localities, which in turn represent strong variation in permeability from non-welded to welded.

After the climax of the Xaltipan ignimbrite eruption, and the Los Humeros caldera collapse, a period of quiescence lasted until *ca*. 70±23 ka ($^{40}Ar/^{39}Ar$, plagioclase: Carrasco-Núñez et al., 2018) with an explosive reawakening producing a sequence of intermittent Plinian eruptions interrupted by soil-marked, repose episodes, named as the Faby Tuff (Ferriz and Mahood 1984; Willcox, 2011). This sequence includes several thick (1-6 m) rhyodacitic coarse-lapilli pumice fallout layers bounded by thin paleosols. Following this explosive phase, a second caldera-forming eruption occurred emplacing the Zaragoza ignimbrite. This is a double compositionally-zoned rhyodacitic-andesitic-rhyolitic single-flow unit, with an estimated volume of ca. 15 km^3 DRE, which produced the 8-10 km Los Potreros caldera (Carrasco-Núñez and Branney, 2005; Carrasco-Núñez et al., 2012b). The age of this eruptive episode was not previously well constrained. Ferriz and Mahood (1984) provided an age of 100 ka (K/Ar, plagioclase) for a lava bellow the Zaragoza ignimbrite, while Willcox (2011) reported a date at 140±24 ka ($^{40}Ar/^{39}Ar$, plagioclase). Recently, Carrasco-Núñez et al. (2018) provided a new $^{40}Ar/^{39}Ar$ (plagioclase) age of 69±16 ka for the Zaragoza ignimbrite, which is supported by the stratigraphic position of the Zaragoza ignimbrite overlying a rhyodacitic lava flow dated at 74.2±4.5 ka (U-Th, zircon).

3.3 Post-Caldera stage

The post-caldera stage is characterized by two different eruptive phases (Carrasco-Núñez et al., 2018).

3.3.1 Late Pleistocene Resurgence phase

This eruptive phase involved the emplacement of relatively small silicic domes within the caldera´s center dated in 44.8±1.7 ka (U-Th zircon; Carrasco-Núñez et al., 2018), which corresponds to a previously dated rock at 60±20 ka (K/Ar whole rock; Ferriz and Mahood, 1984). Some others rhyolitic domes erupted outside the northern sector of the caldera, one of them dated at 50.7±4.4 ka ($^{40}Ar/^{39}Ar$, plagioclase; Carrasco-Núñez et al., 2018). This effusive? activity was followed by several explosive eruptions, originated the Xoxoctic Tuff (0.6 km^3, Ferriz and Mahood, 1984) and an explosive breccia together with pyroclastic flows deposits of the Llano Tuff (Ferriz and Mahood 1984; Willcox, 2011). Charcoal found on an overlaying soil deposit provided a maximum age of 28.3±1.1 ka (C^{14}, Cal BP 30630, Rojas-Ortega, 2016).

3.3.2 Holocene reactivation phase

During the Holocene occurred a volcanic reactivation in the form of explosive and effusive eruptions within the caldera and as ring-fracture volcanism, and as a bimodal phase towards the south, north and central part of Los Humeros caldera (Carrasco- Núñez et al., 2017). Several tens of monogenetic vents erupted in the LHVC (Ferriz and Mahood, 1984; Norini et al., 2015; Carrasco-Núñez et al., 2017b), while some trachyandesitic and andesitic basalts lavas erupted to the north of the LHVC at about 8.9±0.03 ka (C^{14}, Carrasco-Núñez et al, 2017b). Also, a bimodal explosive activity occurred contemporaneously producing both trachyandesitic-dacitic and basaltic fall layers known as the Cuicuiltic Member at 7.3±0.1 ka (C^{14}, Dávila-Harris and Carrasco-Núñez, 2014).).

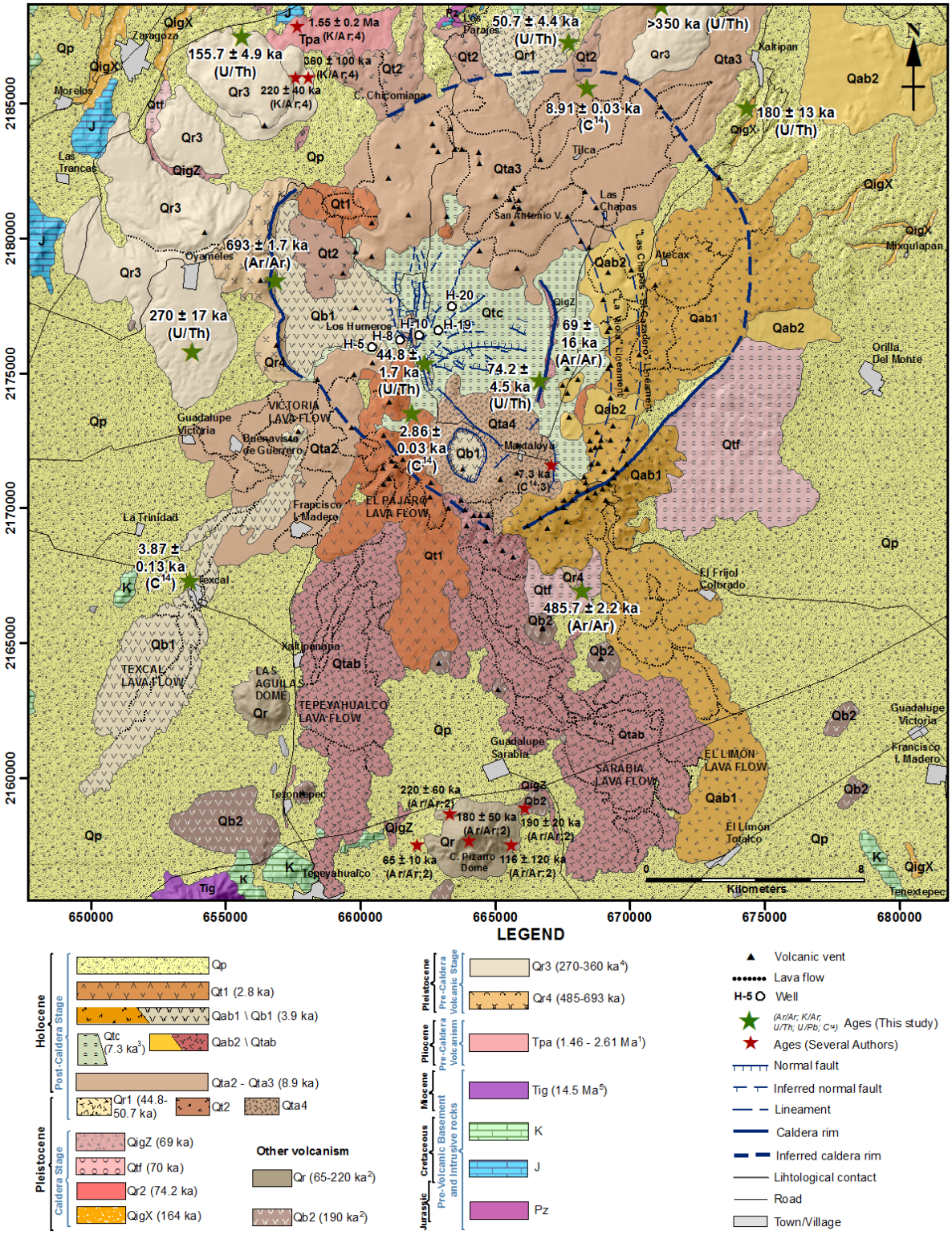

Figure 2: Geologic map of LHVC showing the new main evolution stages (Modified from Carrasco-Núñez et al., 2018).

Finally, a ring-fracture phase occurred towards the southern caldera rim, forming a well-defined lava field that erupted trachyandesites and olivine-bearing basaltic lava flows (Fig. 4), at 3.9±0.13 ka (C^{14}, Carrasco-Núñez et al, 2017b), and a trachytic lava flow at 2.8± 0.03 ka (C^{14}, Carrasco-Núñez et al, 2017b).

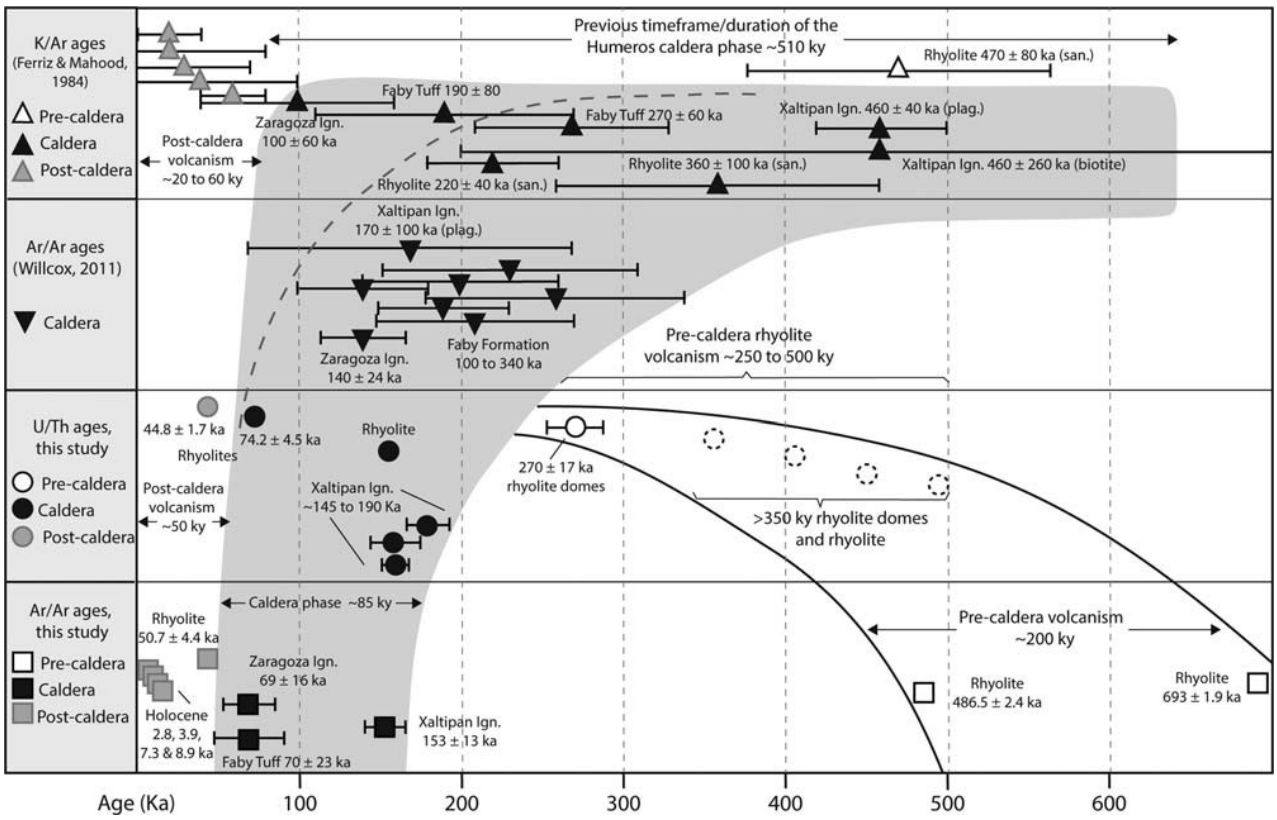

Figure 3: Chronostratigraphy of the LHVC showing the comparison of the recent U/Th and Ar/Ar dating results in Carrasco-Núñez et al. (2018) with the previous works. Note the significant rejuvenation of the caldera stage from 510 to 85 ky.

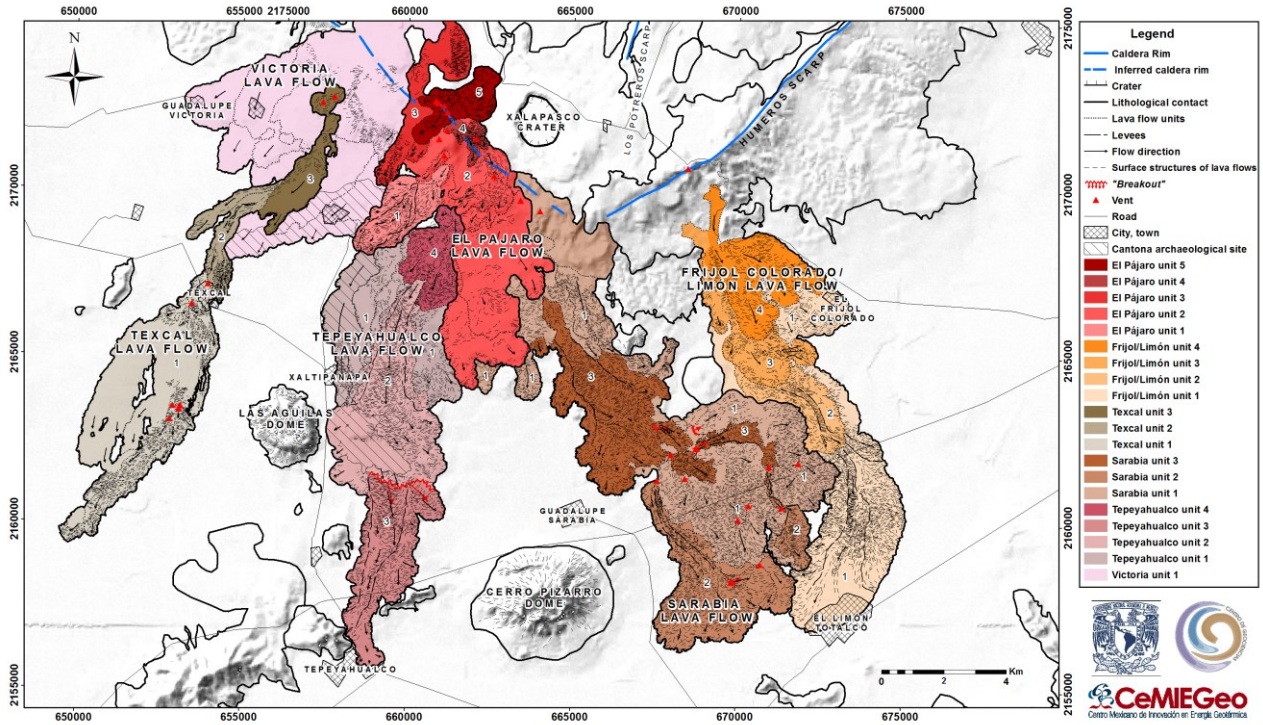

Figure 4: Morphostratigraphic map showing the distribution and relative stratigraphic position of the post-caldera stage Holocene lava field units. Modified from Barrios (2018).

4. STRUCTURAL PATTERNS

4.1 Regional setting

The LHVC basement underwent two main tectonic events: first, the Cretaceous to Paleogene Mexican Fold and Thrust Belt (MFTB) compressional orogeny, with a NE–SW-oriented maximum horizontal stress (σ1) that generated NW–SE-trending thrusts and a major ramp anticline below the LHVC; and second, a minor Neogene-Quaternary extensional tectonic event characterized by NW–SE-oriented minimum horizontal stress (σ3) and NE-SW-trending maximum horizontal stress (σ2), producing discontinuous nearly NE–striking normal faults. The results of the kinematic analysis of the MFTB compressive structures and younger normal faults indicates that the direction of the maximum horizontal stress (first σ1 and then σ2), exerting a control on the direction of magmatic intrusions and transport of fluids in the crust, maintained a constant NE–SW trend during time, suggesting a permutation of the principal stress axis (Norini et al., 2019 in press).

4.2 Volcanotectonic setting

The structural study of the LHVC indicates that the structure of the caldera complex, the local stress field, and the occurrence of hydrothermal fluids in the geothermal reservoir result from the interplay among the heat source (inferred magma intrusion), the recent ground faulting (caldera resurgence) and the intense post-caldera volcanic activity. This interaction caused that the main resurgence faults and post-caldera magma-driven hydrofractures reactivated the inherited tectonic weak planes in the basement underlying the LHVC, leading to the main structures that control the fluids paths (Norini et al., 2019 in press).

Distinct resurgent structural sectors occur within the Los Potreros caldera. The S1 southern structural sector behaves mainly as a single monolithic block uplifted by resurgence, with few shallow E-W faults accommodating minor internal deformations (Figure 5). The S2 northern resurgent sector is affected by normal faults delimiting narrow N-S/NNE-SSW grabens (Figure 5). S3 sector is more stable, not showing evident faulting. These structural features accommodate doming of the topographic surface, inducing uplift of the caldera floor and extension at shallow depths.

Mainly dip-slip displacements (both normal and reverse) occur along the NNW-SSE, N-S, NE-SW and E-W prominent fault strands in the Los Potreros caldera, defining radial displacement vectors centered around

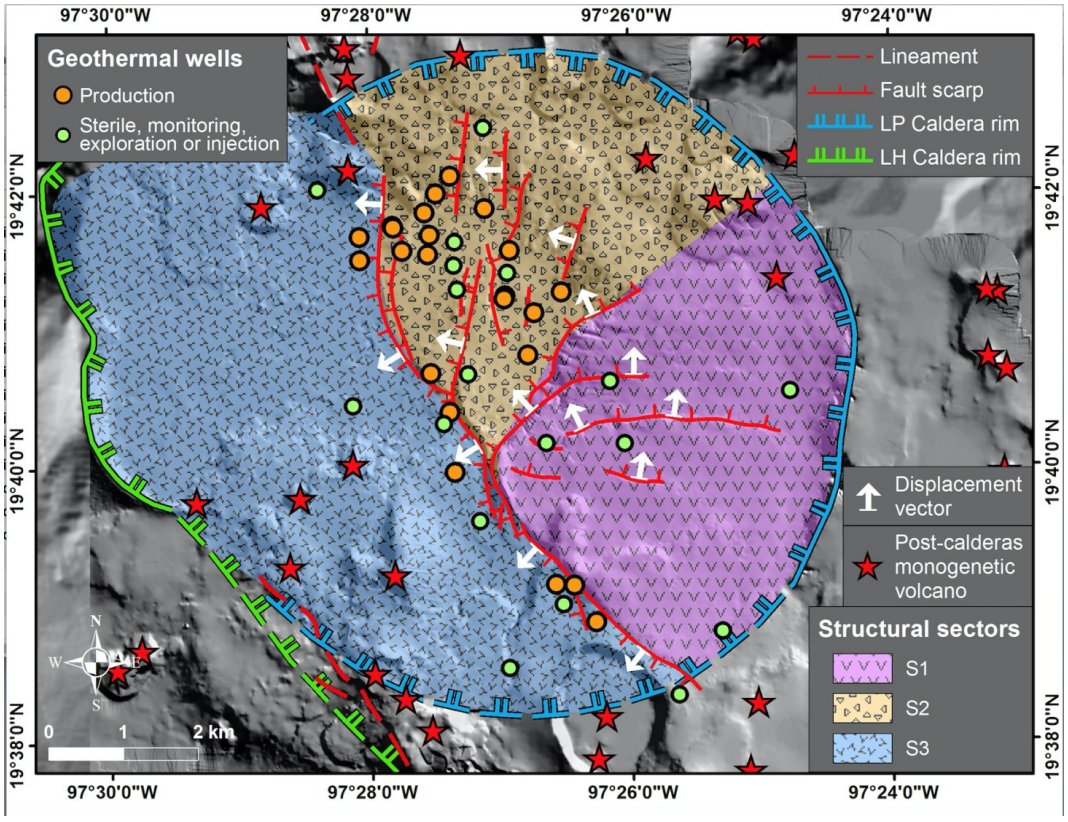

Figure 5: Volcanotectonic patterns showing the cinematic behavior of the three main structural sectors, as proposed by Norini et al. (2015).

5. INTERNAL STRUCTURE

5.1 Subsurface geology

Based on a combination of petrography, geochemistry and $^{40}Ar/^{39}Ar$ geochronology, Carrasco-Núñez et al. (2017a) made a revision of the lithostratigraphy of Los Humeros subsurface, which allow a good correlation with the with the surface geology. The results reveal the highly heterogeneous nature of Los Humeros stratigraphy at depth, responsible for vertical and lateral variations on the permeable conditions that control the geothermal reservoir configuration.

Subsurface geology was organized into four main groups (Carrasco-Núñez et al., 2017a): pre-volcanic, pre-caldera, caldera and post-caldera (Figure 6). The pre-volcanic group correspond to the basement rocks, composed of highly deformed Mesozoic limestone mostly altered forming hornfels and skarn. These rocks are often cut by andesite-like and diabase intrusions with occasional granodiorite. A buried NNW paleostructural system, parallel to the main structural pattern that control the actual geothermal activity has been inferred (López-Hernández, 1995; Cedillo, 1999; Norini et al., 2015). The distribution of the sedimentary basement is highly irregular at depth, being shallower towards the West (see well H-5 in figure 6). Petrologic and geochronologic correlations in this group suggest the development of a complex volcanic field over a highly irregular paleotopographic setting at 1.46-2.61 Ma (Carrasco-Núñez et al., 2017a). This unit is made of voluminous successions of andesitic lava flows derived from different vents with the sporadic occurrence of viscous lava domes. This unit is where the geothermal reservoir is hosted.

The pre-caldera volcanic group includes three andesitic units: a) a basal unit of hornblende-bearing andesites and basalts, b) an intermediate unit of pyroxene-bearing porphyritic andesites that hosts of the geothermal reservoir; and c) an upper unit of rhyolites, dacites domes and andesites. Both the basal and upper units present a restricted lateral distribution, in fact they only appear in well H20 (Fig. 6). The caldera group consists of a thick succession of pyroclastic units. At the base, it includes the Xaltipan ignimbrite, the Los Humeros caldera-forming unit. This intracaldera ignimbrite exhibit contrasting welding variations associated with strong differences in permeability properties. The post-caldera group (< 0.1 Ma) records a diverse volcanic behavior that ranges from effusive to explosive activity and that resulted in a diverse succession of lava flows to fallout deposits with compositions ranging from trachydacites to basaltic andesites.

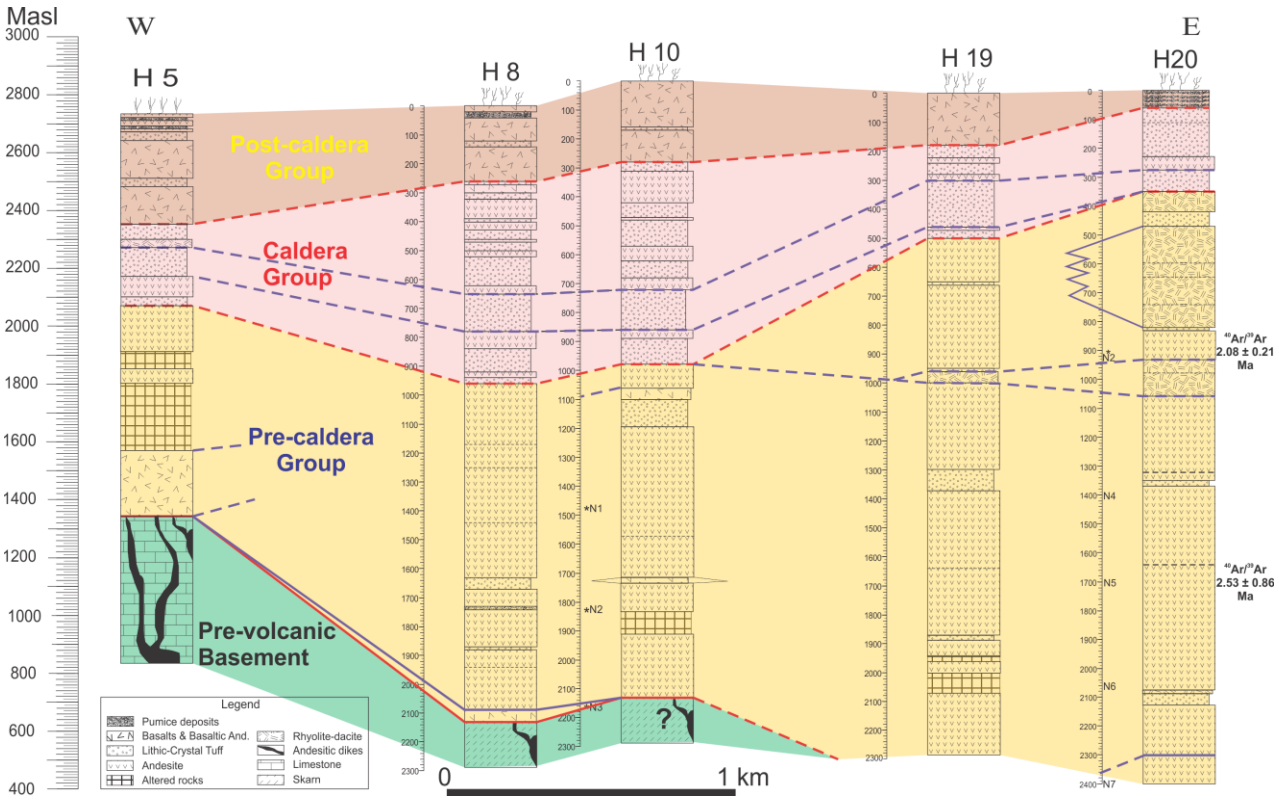

Figure 6: Correlation of the subsurface geology, showing the irregular configuration of the four main geologic groups. Note the thickening of pre-volcanic basement towards the West (well H5). Red lines separated main groups, whereas the blue lines indicate proposed correlation of units within these groups (modified from Carrasco-Núñez et al. (2017). Location of wells in Figure 2

5.1.1 Geochemical correlation of lithostratigraphic units

The irregular distribution and pervasive geothermal alteration of the thick andesitic lava flow succession of the pre-caldera stage difficult the correlation between geothermal wells. Due this, and the usual overlapping problem in volcanic units, we used geochemical signatures to compare and discriminate among different volcanic units in Los Humeros (Carrasco-Núñez et al., 2017a).

To support correlation of the subsurface units we used trace and REE-elements' geochemistry (Nb-La-Sr/Nb). Through the analysis of samples from 12 wells and surface from the pre-caldera group it was possible to differentiate three geochemical groups; for practical purposes named A, B and C. Group A corresponds to the upper unit of the pre-caldera group characterized by rhyolites and dacites (wells H19, H20, H25 and H50) which represents the effusive events associated with large domes. This group is characterized by low Sr/Nb, and moderate to high Nb/La ratio (Figure 7).

The largest group B represents the intermediate unit of the pre-caldera group, which is represented by the Teziutlán andesite present in all the wells studied with values ranging from moderate to high Nb/La and moderate values for the relationship Sr/Nb compared to surface rocks (Figure 7).

Group C correspond to the basal unit of the pre-caldera group, characterized by hornblende-bearing andesitic rocks, located at the bottom of the well H20 and H26. In both wells, the Sr/Nb value is higher compared to the groups A and B (Figure 7). Furthermore, this geochemical signature is consistent with the Miocene rocks of the Cerro Grande volcanic field (CGVF) located ~35 km to the west of the caldera (Gómez-Tuena and Carrasco-Núñez, 2000), thus, a good correlation can be established.

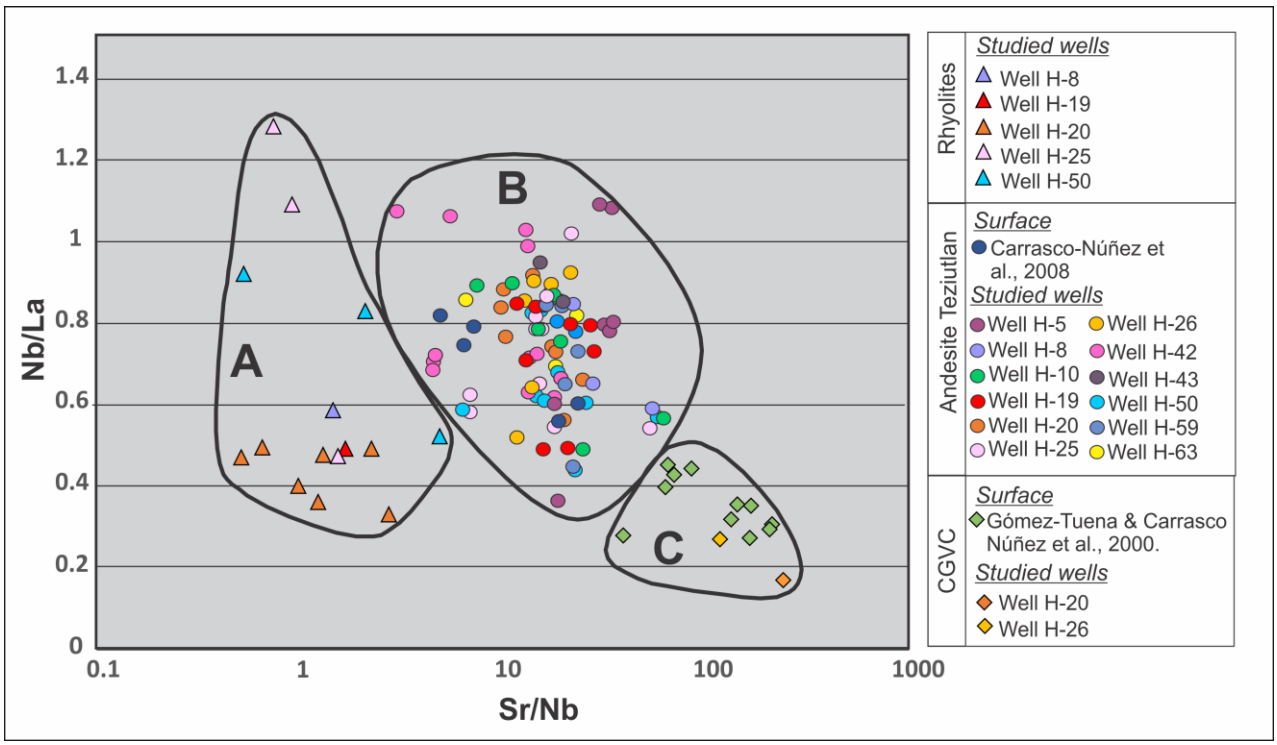

Figure 7: Plot of Sr/Nb vs. Nb/La of the pre-caldera group samples, showing the three geochemical groups A, B and C. Note the correlation of group C with the previously reported geochemical signature of Cerro Grande volcanic field (CGVF) (modified from Carrasco-Núñez et al. (2017a).

5.2 Magmatic plumbing system

The wide compositional range during the post-caldera stage, from basalts to trachytes, suggests the existence of a complex magmatic plumbing system beneath the caldera (e.g., Cashman and Giordano, 2014). A key to decipher where magmas are stored, is the understanding of pre-eruptive processes (such as mineral crystallization), driving evolution, migration and stagnation of melts prior to their eruption (Lucci et al., 2018). As a matter of fact, primary minerals, after their crystallization from the melt, react to the magmatic environment (i.e., pressure – temperature – magma composition) and therefore, constitute with their growth, texture and chemistry, (e.g., Lucci et al., 2018). Accordingly, integration of petrographic observations, primary minerals chemistry, and inverse thermobarometry models lead to the comprehension of the magmatic storage/feeding system associated with erupted products (Lucci et al., 2019 and references therein).

The present-day anatomy of the magmatic plumbing system has been unraveled and reconstructed by integrating petrographic investigations, magmatic textural descriptions and geochemistry characterization (mineral and major-elements bulk-rock chemistry) of thirteen lava samples from Los Humeros post-caldera stage (Carrasco et al., 2017b, 2018) (Lucci et al., 2019). The results can be resumed as:

5.2.1 Basalts

Plagioclase-liquid and olivine-liquid thermobarometric models applied to phenocryst compositions indicate for all basaltic material an anhydrous temperature of *ca.* 1230-1270 °C at *ca.* 8 kbar (Figure 8a,b). Clinopyroxene, where present, recorded a polybaric evolution and migration of basaltic melts within the crust (Figure 8b). Groundmass and aegirine-rich pyroxenes indicate lower temperatures (1060-1100°C) at superficial conditions (0.5-2.0 kbar) (Figure 8b).

5.2.2 Trachyandesites

All studied trachyandesites (Figure 8c) show a continuous of temperatures from ca. 1250°C (plagioclase phenocryst cores) to 950-1000°C (groundmass clinopyroxenes) with crystallization depth spanning from 9 kbar (comparable to basalt depths) to 0.5 kbar (superficial crystallization). Furthermore, Opx-bearing trachyandesites show orthopyroxene-liquid equilibria verified for very superficial hot conditions (1050-1100°C at 0.5-2.5 kbar).

5.2.3 Trachytes

Magmatic P-T conditions, obtained for trachytes (Figure 8d), are characterized by plagioclase crystallization between 1050-1100°C at depth of 5-9 kbar (comparable to those of trachyandesites) and by very shallow crystallization conditions between 900-1000°C at

0.2-3 kbar. The occasional presence of orthopyroxene (Opx), can be considered a tracer of magma stagnations at shallow depth, since the invariably lower pressure values obtained by Opx-liquid barometer.

These results indicate that, unlike previously believed, the present configuration of the plumbing system is vertically extensive, crossing the entire crust with a deeper residence zone for basalts at 8 kbar (ca. 30 km). Also, is interpreted a complex middle to very? upper crust zone (0.5 kbar), where smaller batches of magma differentiate to trachyandesites and trachytes at times interconnected with the lower feeding zone.

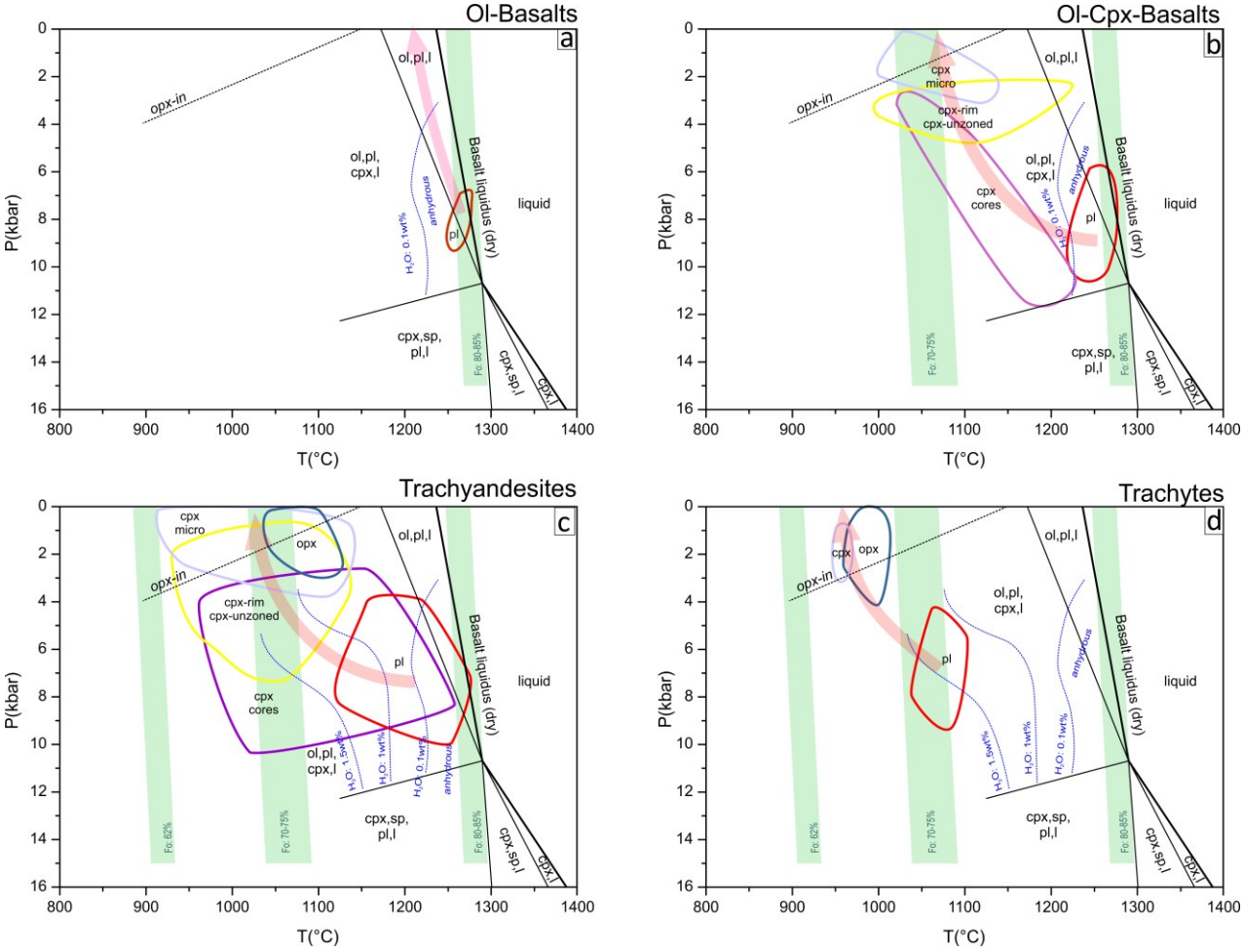

Figure 8: Pressure-Temperature diagrams as derived from inverse thermobarometry models applied to Los Humeros post-caldera stage lavas. P-T diagrams show a polybaric magmatic system compatible with a multilayered magmatic feeding system vertically distributed in the whole crust beneath the Los Humeros caldera. a) Olivine-bearing Basalts; b) Olivine-clinopyroxene basalts; c) Trachyandesites; d) Trachytes. Key for minerals: ol-olivine, pl-plagioclase, opx, orthopyroxene, cpx-clynopyroxene, sp, spinel.

In summary, as a result of these thermobarometry models a polybaric magmatic system is interpreted, supporting a configuration with multiple magmatic stagnation levels that fed different eruptive episodes forming the post-caldera volcanism of Los Humeros caldera.

6. IMPLICATIONS FOR THE GEOTHERMAL SYSTEM

6.1 Permeability of the geothermal system

6.1.1 Fracture-dominated paths and recharge

The preferential trends of the mafic intrusions in the pre-caldera sedimentary basement suggest that fluids in the crust moved along two orthogonal preferential directions: 1) a NW–SE-trending weak planes, coinciding with sedimentary bedding and inherited MFTB folds and faults; and 2) a NE–SW-trending maximum horizontal stress and normal faults. These trending directions may also control the flow and recharge paths of groundwater.

The recent volcanotectonic deformations inside the Los Potreros caldera, induced by the active resurgence activity, are inferred to control the secondary permeability within the Los Humeros geothermal field and should be regarded as the most important targets for geothermal exploration. The geometry of these deformation features is partly inherited from pre-existing, regional tectonic structures, where the radial stress field caused by the active magmatic system control the strike of hydrofractures, with the expected geometry of faults and fractures (Norini et al., 2019: in press).

6.1.2 Microporosity

Permeability of geothermal systems has usually been associated mainly to faults and fractures, underestimating the possible contribution of porosity connected pathways referred as microporosity. In order to present a more realistic permeability model that includes the microporosity, seven andesite samples from a production well (see location in figure 2) were analyzed through X-ray Micro-Computed Tomography (μCT) following the methodology described by Cid et al., (2017). All samples were imaged using a resolution of 0.5 μm^3. Pores greater than 0.5 μm (macropores) were segmented using Otsu's thresholding algorithm, resulting in a relatively low porosity volume fraction averaging less than 4% and without showing any relevant connectivity. Therefore, macropores do not provide real flow channels that will account for permeability, maybe the reason why porosity has been discarded before. Micropores (pores below 0.5 μm resolution) on the other side, average more than 6% porosity, which added to macropores can account for up to 15% of total porosity (Fig. 9c). Furthermore, microporosity in most cases acts as links between the bigger pores, enhancing pore network connectivity, reaching in some cases more than 70% of connected pores. Figure 9a shows the characteristic distribution of the intermediate region (micropores) along andesite samples. The gray intensity is related to the amount of void within the pixel, black pixels correspond to macropores while white correspond to the solid phase. It can be observed that gray zones are usually near or inside to macropores. The micropore volume distribution was then calculated showing a median volume of 8.97 μm^3 (Fig. 9b). The peak is near 2 μm^3 showing only the right tail of the distribution which means that half of the micropores are between 0 and 2 μm^3. Once total porosity was calculated, the connected pore model was extracted by selecting a threshold value corresponding to the grey-scale level of porosity percent. Subsequently, flow simulations were computed on the processed images, calculating the absolute permeability, velocity and pressure fields solving Navier-Stokes Equations with a Finite Volume Method. Darcy's law was then used to calculate absolute permeability in the *z* direction. In general, results show permeability in a range between 0.1 and 1.5 mD (Figure 9d).

Results of total porosity (macro + micro) and permeability reveal a zone with no effective porosity between 1,000 and 1,200 m, likely sealing the reservoir. Also, is observed a relatively high porosity for samples between 1,400 and 2,200 m, which indicates the probable location of the reservoir. Looking at permeability, different results were obtained for samples with similar porosity (that ranges from 12-15%), indicating a variation on pore network properties. Properties such as pore and throat radius, tortuosity, sphericity, coordination number, define the shape of porosity pathways, which are determining in flow and rock permeability. A peak on permeability was identified in the zone between 1,700 and 2,400 m falling inside the well permeable zone. In general, a good correlation exists between the computed porosity permeability and the well-logs, indicating that porosity particularly the micropore fraction provide effective flow pathways that enhance reservoir permeability. Even with a relative low permeability, microchannels are able to transport the highly pressured water steam of the vapor-dominated reservoir, with an effective traveling through small cavities. Condensation may take place in pore walls, however the high exchange of geothermal heat fosters evaporation, allowing a continuous flow along micropores. Our findings suggest that porosity, particularly microporosity have a contribution on the permeability of Los Humeros geothermal reservoir of around 1-3 mD, together with cracks and faults. These analyses are necessary during the exploration stage for an accurate permeability model.

6.2 Cap rock

The Xáltipan ignimbrite represents the major explosive eruption of the LHVC, that derived in the Los Humeros caldera collapse (Ferriz and Mahood, 1984). This ignimbrite has >291 km^3 (DRE) volume, that emplaced in the form of mainly consolidated intracaldera deposits (55 km^3) and as widespread outflows (236 km^3) (Figure 10a) (Cavazos and Carrasco-Núñez, in review). Inside the caldera, this unit present important thickness values (90 - 880 m), and covers massively the highly-fractured andesite basement, which is inferred to host the reservoir rock of the geothermal system. Due to the occurrence of consolidated samples obtained from the drilling process and its stratigraphic position, this unit has been referred as a homogenous unit with low to null permeability that acts as the caprock of the system (Cedillo, 1999). Nevertheless, recent geological characterization of the outer and intracaldera deposits of this ignimbrite has revealed abrupt lithofacies variations caused mainly by welding processes and secondary mineralization (Cavazos et al., in review) (Figure 10). This suggest that the ignimbrite is highly heterogeneous and present textural changes that modifies permeability. New studies on the outer and intra caldera deposits, integrating petrographic (thin-section) and petrophysical analyses (μCT and He-permeometry) shows that permeability goes in a range from practically null, to highly permeable (0.001 – 1,500 mD), and that that porosity and permeability are in fact spatially variable in the order of a few tens of meters. These variations are determined by multiple factors associated with the welding development and precipitation of secondary processes such as argillic alteration of glass and secondary mineralization in the pore fraction.

Welding degree of the Xáltipan ignimbrite goes in a wide spectrum from rank I-VI (Quane and Russel, 2005), and is probably the most important factor controlling permeability. Here, the non-welded (rank-I) zones presents high pore volume of >50% and permeability of >1,500 mD. In contrast, highly welded lithofacies shows a pore reduction by compaction of 5-6% and practically null permeability values of 0.001 mD (Cavazos et al, in review). Also, secondary mineralization is observed in the moderately to non-welded facies, particularly argillic alteration and crystal growth (quartz) in the pore walls reducing the pore connectivity. These observations are consistent with geophysical studies that show spatial resistivity anomalies along the Xáltipan deposits, and that is interpreted that occur due zones of high conductivity due to argillic alteration and ilite-smectite precipitation. These observations contradict the conventional idea that suggest that the Xáltipan ignimbrite is spatially homogeneous and that acts as caprock of the geothermal system. In conclusion, the Xáltipan ignimbrite is a heterogeneous rock, with variable lithofacies that change abruptly and that control the permeability of the rock (Fig. 10b), being welding and secondary mineralization the most relevant.

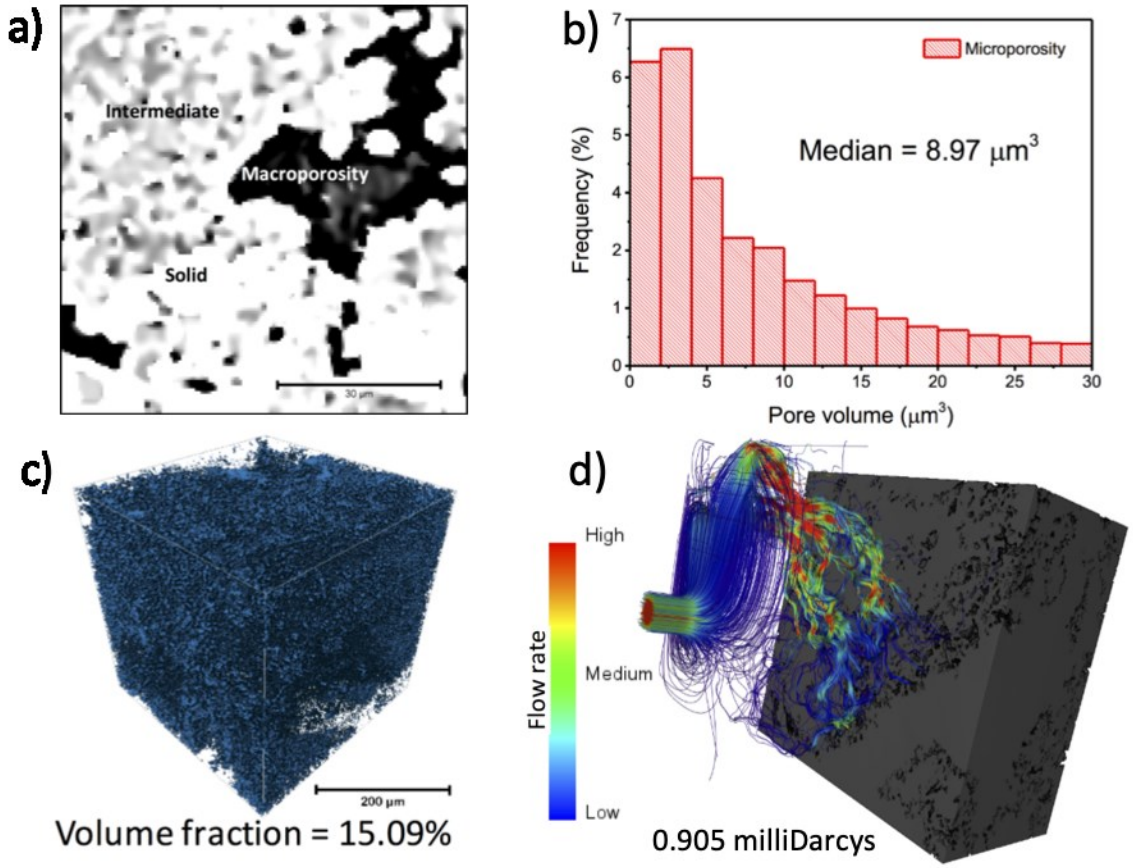

Figure 9: Porosity and permeability analysis. (a) µCT image showing the intermediate zone (gray) where micropores are embedded in solid matrix. (b) Pore volume distribution showing the median for the micropores. (c) 3D representation of connected porosity including both macro and micropores. (d) Graphical representation of the flow velocity field result of a permeability simulation. (Modified from Cid et al., 2017).

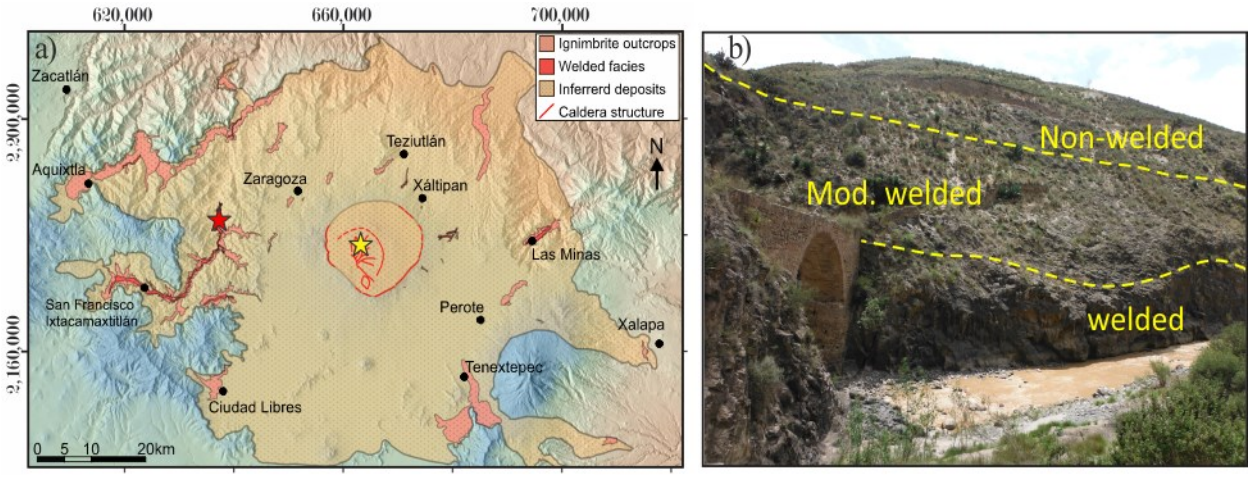

Figure 10: Lithofacies of the Xaltipan ignimbrite. a) Digital Elevation Model showing the distribution of the major-caldera forming event of the LHVC (Xaltipan ignimbrite); the red star indicates location of picture "b"; b) Photograph showing the variations of welded facies in the same outcrop. Bridge is 7m scale as reference for scale.

6.3 Heat source

The results presented in section 5.2 indicate a current multilayered configuration of the plumbing system extending across the entire crust from 8 kbar (ca. 30 km) to about 0.5 kbar, with relatively small magma batches from different compositions emplaced at times interconnected with the lower feeding zone. The main outcome for the modeling of the geothermal magmatic heat source is the inadequacy of conservative conceptual models based on the classical melt dominated, single, voluminous, long-lived magma chamber (i.e. the Standard Model in Gualda and Ghiorso, 2013) as envisaged so far at LHVC (e.g. Verma et al 2011). Instead, new and more realistic vision of magmatic plumbing systems made of multiple interconnected and parcellized magma stagnation layers within the crust have been proposed recently (e.g., Cashman and Giordano, 2014). The availability of a new and better refined geochronology (Carrasco-Núñez et al., 2018) allows the reconstruction of the main recent evolutive phases of the magma heat

source, which can be summarized as it follows. During the caldera stage, from the eruption of the Xáltipan ignimbrite to the eruption of the Zaragoza ignimbrite (164 to 69 ka), a liquid dominated magma chamber existed at ~5 km depth (Ferriz and Mahood, 1984), dominated by rhyolitic compositions with andesitic zonation (Carrasco and Branney, 2005). The two caldera-forming eruptions depleted largely this magma chamber from the melt phase, and since 69 ka there is no evidence for a large liquid-dominated lens, as indicated by the eruption of all possible compositions from the caldera floor in close space and time frames (Lucchi et al., 2019); we therefore propose that the crystallized part of the large magma chamber of the caldera stage has not been recharged and is presently cooling. The ongoing post-caldera stage is characterized instead by a better localized and scattered small volume magma batches that intruded at various times and depths, suggesting a much more complex geometry for the magmatic heat source(s). This multilayered magmatic system may include stagnation levels locally as shallow as to be intruded within the geothermal reservoir and caprocks (Urbani et al., 2019).

6.4 3D model

The geological and geophysical 3D model of the Los Humeros caldera was generated based on geological information obtained by well-logging and the surficial information from the geological maps (Carrasco-Núñez et al., 2017b) and by using the LeapFrog Geo software. Additionally, the geophysical data obtained from electromagnetic (MT) (Figure 11), gravimetric and seismicity methods were used to define the main geological structures.

The integrated results of these multidisciplinary studies provide a preliminary 3D visualization of the geological and structural setting of the caldera. This permits a more comprehensive reconstruction of the volcanic complex, ejected magma volumes, and a more direct correlation of the parameters intervening in the geothermal system.

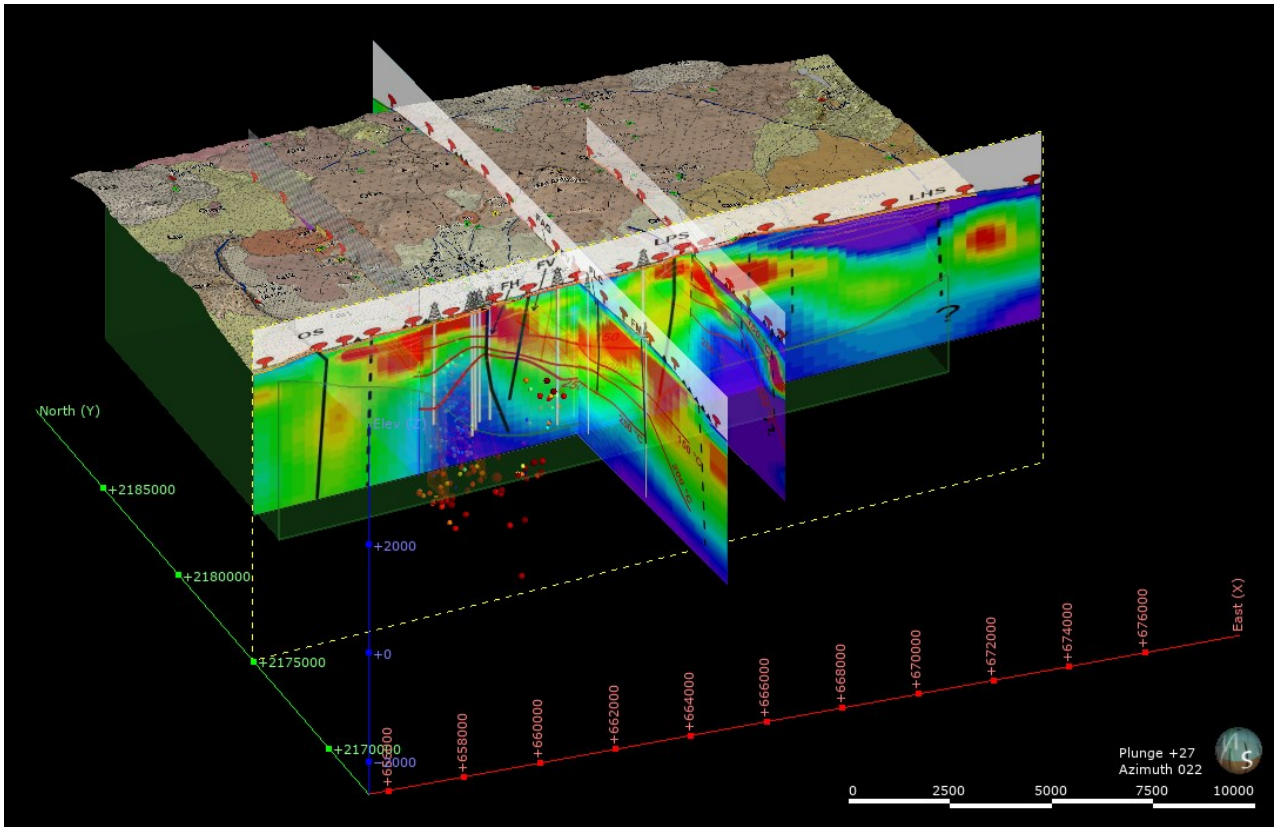

Figure 11: 3D geological and geophysical model of Los Humeros caldera. Here, MT profiles (Arzate et al., 2018) were compared with surficial and subsurface geology for correlation of the faulting system, alteration zones, temperature, seismicity among other parameters.

7. CONCLUSIONS

We propose an integrated approach to understand the volcanologic, magmatic and structural evolution of LHVC as a good example to unravel the general behavior of Superhot geothermal systems (SHGS), as a basis to explain how the geothermal system develops through time.

The volcanotectonic evolution of LHVC has been very complex, involving cataclysmic episodes of caldera-forming and plinian eruptions produced during the caldera stage. This evolution is now better constrain with new geochronologic dating within a period of 69 to 164 ky (Carrasco-Núñez et al, 2018). The internal structure of the caldera was modelled following a combination of dominantly trapdoor and less piecemeal caldera types, in addition of inherited structures from previous geological episodes as the caldera was built on a highly folded and fractured sedimentary basement. The paleotopography of this regional basement was partially covered by a thick sequence of andesitic followed by rhyolitic dome volcanism.

The structural analysis suggests that NW-SE and NE-SW-trending regional tectonic patterns structures are dominant in the basement and pre-caldera volcanic rocks. The structural integrity of LHVC was also affected the nature of the caldera-forming structure and the evolution of the magma feeding system, during the post-caldera stage, which culminated with the resurgence of the magmatic system. During this process, reactivation of resurgence faults and post-caldera magma-driven hydrofractures generated under a local radial stress field from the interplay among the heat source (inferred magma intrusion), the recent ground faulting (caldera resurgence) and intense post-caldera volcanic activity. This recent active resurgence of the caldera, may control the secondary permeability within the geothermal field and should be considered very important for geothermal exploration. It is possible that part of the geometry of these deformation features is apparently inherited from pre-existing, regional tectonic structures.

A complex multilayered configuration of the magmatic plumbing system is inferred from thermobarometry models, indicating a polybaric magmatic system, with different levels of magma stagnation, which have been particularly active during the post-caldera stage, in the Holocene, through different eruptive successions erupted mostly to the south as ring-fracture lava flow and within the caldera. These results suggest that the present configuration of the plumbing system occupies an extensive zone ranging from a deeper residence zone for basalts at 8 kbar (ca. 30 km) up to very shallow zone (0.5 kbar), with a complex middle crust zone where smaller batches of magma differentiate to trachyandesites and trachytes, which are in many cases interconnected with the lower feeding zone. We consider that a recurrent injection of magmas occurred until the Holocene, associated with a diversification of the magmatic sources and their interaction with the geothermal system.

Regarding the permeability of the geothermal system, it is clear that fractures have a major control on it, however, an important contribution must be provided by primary vesiculation (microporosity) of the volcanic rocks, as shown in this study.

Internal variations in permeability observed in LH the geothermal reservoir within the caldera through the study of the geothermal wells, could be explained in part considering the heterogeneous variations in lithofacies such as those observed in the degree of welding of the Xaltipan ignimbrite, as they are in direct correlation with permeability (welded-impermeable; non-welded-highly permeable). Furthermore, correlation based on geochemistry of immobile trace and REE elements help us to refine the subsurface stratigraphy and correlation with the surficial geology and then refine the geologic model.

The final 3D model presented here, allows us to make visual correlations of the different parameters involved in the geothermal system and all different type of information (geology, geophysics and geochemistry) in order to establish a better understanding of the conditions that characterize the geothermal field of LHVC.

ACKNOWLEDGEMENTS

This paper presents results of the GEMex Project, funded by the Mexican Energy Sustainability Fund CONACYT-SENER, Project 2015-04-268074 (WP 4.5), and by the European Union's Horizon 2020 research and innovation program under grant agreement No. 727550. G. Carrasco is grateful to the PASPA-DGAPA program (UNAM) for support during his sabbatical stay at the University of Toma Tre (Rome, Italy).

REFERENCES

Arellano, V.M., García, A., Barragán, R.M., Izquierdo, G., Aragón, A., Nieva, D., 2003.An updated conceptual model of the Los Humeros geothermal reservoir (Mexico). J. Volcanol. Geotherm. Res. 124, 67–88.

Arredondo, J.F., 2007. Integración geofisica en el campo geotérmico de LosHumeros. Internal report CFE GF-HU 02-07.

Arzate, J., Corbo, F., Norini, G., Carrasco-Núñez, G., Hernández, J., Yustis, V., 2018. The Los Humeros (Mexico) geothermal field model deduced from new geophysical and geological data. Geothermics, 71, 200-211. http://dx.doi.org/10.1016/j.geothermics.2017.09.009.

Barragán, R.M., Nieva, D., Santoyo, E., Verma, M.P., Izquierdo, G., González, E., 1991.Geoquámica de fluidos del campo geotérmico de Los Humeros, Pue. (Mexico). Geotermia 7, 23–47.

Barrios, S, 2018. Caracterización morfológica de los derrames del campo de lava de Los Humeros, Puebla. Tesis de licenciatura, Instituto Tecnológico de Cd. Madero. 45 pp.

Campos-Enriquez, J.O., Garduño-Monroy, V.H., 1987. The shallow structure of Los Humeros and Las Derrumbadas geothermal fields, Mexico. Geothermics 16(5/6), 539-554.

Carrasco-Núñez, G., Gómez-Tuena, A., Lozano, V.L., 1997. Geologic map of Cerro Grande volcano and surrounding area, Central Mexico. Geol. Soc. Am. Map Chart Ser. MCH 081, 10 p.

Carrasco-Núñez, G., Branney, M., 2005. Progressive assembly of a massive layer of ignimbrite with normal-to-reverse compositional zoning: the Zaragoza ignimbrite of central Mexico. Bulletin of Volcanology, 68, 3-20.

Carrasco-Núñez, G., Dávila-Harris, P., Riggs, N.R., Ort, M.H., Zimmer, B.W., Willcox, C.P., and Branney, M.J., 2012, Recent explosive volcanism at the Eastern Trans-Mexican Volcanic Belt, in Aranda-Gómez, J.J., Tolson, G., and Molina-Garza, R.S., eds., The Southern Cordillera and Beyond: Geological Society of America Field Guide 25, p. 83–113, doi:10.1130/2012.0025(05).

Carrasco-Núñez, G., McCurry, M., Branney, M.J., Norry, M., Willcox, C., 2012. Complex magma mixing, mingling, and withdrawal associated with an intraplinian ignimbrite eruption at a large silicic caldera volcano: Los Humeros of central Mexico. Geological Society of America Bull 124, 1793–1809.

Carrasco-Núñez, G., López-Martínez, M., Hernández, J., & Vargas, V. (2017a). Subsurface stratigraphy and its correlation with the surficial geology at Los Humeros geothermal field, eastern Trans-Mexican Volcanic Belt. Geothermics, 67, 1-17.

Carrasco-Núñez, G., Hernández, J., De León, L., Dávila, P., Norini, G., Bernal, J. P., Jicha, B., Navarro, M., & López-Quiroz, P. (2017b). Geologic Map of Los Humeros volcanic complex and geothermal field, eastern Trans-Mexican Volcanic Belt/Mapa geológico del complejo volcánico Los Humeros y campo geotérmico, sector oriental del Cinturón Volcánico Trans-Mexicano. Terradigitalis, 1, 1-11. DOI: 10.22201/igg.terradigitalis.2017.2.24.78.

Carrasco-Núñez, G., Bernal, J. P., Davila, P., Jicha, B., Giordano, G., & Hernández, J. (2018). Reappraisal of Los Humeros volcanic complex by new U/Th zircon and 40Ar/39Ar dating: Implications for greater geothermal potential. Geochemistry, Geophysics, Geosystems, 19(1), 132-149.

Cashman, K. V., & Giordano, G. (2014). Calderas and magma reservoirs. Journal of Volcanology and Geothermal Research, 288, 28-45.

Cavazos, J., Carrasco-Núñez, G., 2017. Vertical and lateral variations of a caldera-related ignimbrite and their implications in an active geothermal system: The case of Los Humeros geothermal field, Mexico. IAVCEI 2017, Portland, USA. Abstract volume.

Cavazos, J., Carrasco-Núñez, G., 2019. Anatomy of the largest (ca. 285 km3) eruption of the Trans-Mexican Volcanic Belt, the Xáltipan ignimbrite from Los Humeros Volcanic Complex, Mexico, implications for greater geothermal conditions. Journal of Volcanology and Geothermal Research (in review)

Cedillo, F., Viggiano, J.C. and Gutiérrez-Negrín, L.C., 1994. Columnas Petrográficas delos Pozos Geotérmicos de Los Humeros. Internal report, Comisión Federal deElectricidad. México, 197 pp.

Cedillo, F., 1997. Geología del subsuelo del campo geotérmico de Los Humeros, Pue., Internal report, Comisión Federal de Electricidad, México. 30 pp.

Cedillo, F., 1999. Modelo hidrogeológico de los yacimientos geotérmicos de Los Humeros, Pue., Mexico. Geotermia, Revista Mexicana de Geoenergía 15-3, 159-170.

Cid, H.E., Carrasco-Núñez, G., Manea, V., 2017. Improved method for effective rock microporosity estimation using X-ray microtomography. Micron, 97, 11-21. http://dx.doi.org/10.1016/j.micron.2017.01.003.

Dávila-Harris, P., Carrasco-Núñez, G., 2014. An unusual syn-eruptive bimodal eruption: the Holocene Cuicuiltic Member at Los Humeros caldera, Mexico. Journal of Volcanology and Geothermal Research 271, 24–42.

De la Cruz, V., 1983. Estudio geológico a detalle de la zona geotérmica Los Humeros, Puebla. (Internal Rep. 10/83, pp. 51). Mexico City: Comisión Federal de Electricidad.

Ferriz, H., y Mahood, G., 1984. Eruption Rates and Compositional Trends at Los Humeros Volcanic Center, Puebla, Mexico. Journal of Geophysical Research, 89, B10, 8511-8524.

Ferriz, H., Mahood, G., 1987. Strong compositional zonation in a silicic magmatic system Los Humeros, Mexican Neovolcanic Belt. J. Petrol. 28, 171–209.

Garduño-Monroy, V.H., Romero, F., Torres, R., 1985. Análisis estructural del campogeotérmico de Los Humeros. CFE, Internal report, Pue. (México) 26–85.

Garduño-Monroy, V.H. and Vargas, L.H., 1987. Análisis de teledetecci6n y bibliográfico del sector de Tres Virgenes, B.C.S. Fieldwork program, Intern. Rep. GG 8/ 87, Gerencia de proyectos Geotermoeléctricos-CFE (Mexico), 34 pp.

Gómez-Tuena, A., Carrasco-Núñez, G., 2000. Cerro Grande volcano: the evolution of a Miocene stratocone in the early Trans-Mexican Volcanic Belt. Tectonophysics 318 (1), 249–280, doi: 10.1016/S0040-1951(99)00314-5. URL: http://www.sciencedirect.com/science/article/pii/ S0040195199003145.

Gualda, GAR, Ghiorso, MS., 2013. The Bishop Tuff giant magma body: An alternative to the Standard Model. Contributions to Mineralogy and Petrology. 166(3):755-775. DOI: 10.1007/s00410-013-0901-6.

Gutiérrez-Negrín, 2019. Current status of geothermal-electric production in Mexico. IOP Conf. Ser.: Earth Environ. Sci. 249 012017. doi:10.1088/1755-1315/249/1/012017

Gutiérrez-Negrín e Izquierdo-Montalvo, G., 2010. Review and update of the main features of the Los Humeros geothermal field, Mexico. Proccedings World Geothermal Congress, Bali, Indonesia, april 2010.

Lermo, J., Antayhua, Y., Quintanar, L., Lorenzo, C., 2008. Estudio sismológico del campo geotérmico de Los Humeros, Parte I, Sismicidad, mecanismos de fuente y distribución de esfuerzos. Geotermia 21, 25-41.

López-Hernández, A., 1995. Estudio Regional Volcánico y Estructural del Campo Geotérmico de Los Humeros, Puebla., México. Geotermia, Revista Mexicana de Geoenergía 11 (1), 17–36.

Lorenzo-Pulido, C.D., 2008. Borehole geophysics and geology of well h-43, Los Humeros geothermal field, Puebla, México. Geothermal Training Programme Report. 9. Orkustofnun, Grensásvegur, Reykjavík, Iceland, p. 23.

Lucci, F., Rossetti, F., Becchio, R., Theye, T., Gerdes, A., Opitz, J., Baez, W., Bardelli, L., De Astis, G., Viramonte, J., & Giordano, G. (2018). Magmatic Mn-rich garnets in volcanic settings: Age and longevity of the magmatic plumbing system of the Miocene Ramadas volcanism (NW Argentina). Lithos, 322, 238-249.

Lucci, F., Carrasco-Núñez, G., Rossetti, F., Theye, T., White, J. C., Urbani, S., Azizi, H., Asahara, Y., and Giordano, G.: Anatomy of the magmatic plumbing system of Los Humeros Caldera (Mexico): implications for geothermal systems, Solid Earth Discuss., https://doi.org/10.5194/se-2019-86, in review, 2019.

Norini, G., Groppelli, G., Sulpizio, R., Carrasco-Núñez, G., Davila-Harris, P., Pellicioli, C., Zucca, F., De Franco, R., 2015. Structural analysis and thermal remote sensing of the Los Humeros Volcanic Complex: Implications for volcano structure and geothermal exploration, Journal of Volcanology and Geothermal Research 301, 221-237.

Norini, G., Carrasco-Núñez, G., Corbo, F., Lermo, J., Hernández, J., Castro, C., Bonini, M., Montanari, D., Corti, G., Moratti, G., Piccardi, L., Chavez, G., Zuluaga, M.C., Ramírez, M., Cedillo, F., 2019. The structural architecture of the Los Humeros volcanic complex and geothermal field. Journal of Volcanology and Geothermal Research, in press. Doi.org/10.1016/jvolgeores.2019.06.010.

Palacios-Hertweg, L., García-Velázquez, H., 1981. Informe Geofísico Del ProyectoGeotármico Los Humeros Derrumbadas, Estados De Puebla Y Veracruz. InternalReport, Comisién Federal de Electricidad, pp. 96.

Perez-Reynoso, J., 1978. Geolog ıa y petrograf ıa de Los Humeros. Geomimet, 91, 97–106.

Prol, R.M., 1998. Pre- and post-explotation variations in hydrothermal activity in Los Humeros geothermal field, Mexico. J. Volcanol. Geotherm. Res. 83, 313–333.

Quan, S. L., Russell, J.K., 2005. Ranking welding intensity in pyroclastic deposits. Bulletin of Volcanology. 67(2):129-143. DOI: 10.1007/s00445-004-0367-5.

Rojas, O., E., 2016. Litoestratigrafía, petrografía, y geoquímica de la Toba Llano, y su relación con el cráter El Xalapazco, Caldera de Los Humeros, Puebla. MSc. Thesis, IPYCYT, México.

Urbani, S., Giordano, G., Lucci, F., Rossetti, F., Acocella, V., and Carrasco-Núñez, G.: Estimating the depth and evolution of intrusions at resurgent calderas: Los Humeros (Mexico), Solid Earth Discuss., https://doi.org/10.5194/se-2019-100, in review, 2019.

Verma, S.P., 1983. Magma genesis and chamber processes at Los Humeros caldera, Mexico—Nd and Sr isotope data. Nature 302, 52–55. Verma, S.P., 2000. Geochemical evidence for a lithospheric source for magmas from Los Humeros Caldera, Puebla, Mexico. Chem. Geol. 164, 35–60.

Verma, S.P., 2000. Geochemical evidence for a lithospheric source for magmas from Los Humeros Caldera, Puebla, Mexico. Chem. Geol. 164, 35–60.

Verma, S.P., Gómez-Arias, E., Andaverde, J., 2011, Thermal sensitivity analysis of emplacement of the magma chamber in Los Humeros caldera, Puebla, Mexico, International Geology Review, Volume 53, Pages 905-925

Viggiano, J.C., Robles, J., 1988. Mineralogía hidrotermal en el campo geotérmico de Los Humeros, Pue.: sus usos como indicadora de temperatura y del régimen hidrológico. Geotermia, Revista Mexicana de Geoenergía, 4, 15-28.

Viggiano, J.C., Flores-Armenta, M., 2008. Estudio petrográfico del pozo H 43 Los Humeros, Pue., interpretación e indicadores mineralógicos de acidez. Internal report C.F.E., DEX, DGL-HM-01-08. 30 pp.

Viniegra, F., 1965. Geología del Macizo de Teziutlán y la Cuenca Cenozoica deVeracruz. Asociación Mexicana de Geólogos Petroleros, Boletín 17, 101–163.

Yáñez, C. and García, S., 1980. Exploración de la región geotérmica Los Humeros-Las Derrumbadas, Estados de Puebla y Veracruz. C.F.E., Internal report 96 pp.

Yáñez, C. and García, S., 1982. Exploración de la región geotérmica Los Humeros-Las Derrumbadas, Estados de Puebla y Veracruz (Internal report, pp. 1–96). Mexico City: Comisión Federal de Electricidad.

Willcox, C. 2011. Eruptive, magmatic and structural evolution of a large explosive caldera volcano: Los Humeros México. PhD thesis, University of Leicester, U.K.